Ultrasound to improve both synthesis and pollutants degradation based on metal nanoparticles supported on TiO_2

M. Stucchi,[1] G. Cerrato[2,3] and C.L. Bianchi[1,3]*.

[1]*University of Milan, Chemistry Department, Via Golgi 19, 20133, Milano, Italy.*

[2]*University of Turin, Chemistry Department, Via P. Giuria 7, 10125, Torino, Italy*

[3]*Consorzio INSTM, Firenze, Italy*

**Claudia.bianchi@unimi.it*

Abstract

Sonochemistry is based on acoustic cavitation, which consist in the formation, growth, and implosive collapse of bubbles within a liquid. Collapsing bubbles generate localized hot spots, characterized by temperatures up to 5000 K and pressures up to 1800 atm. These extreme conditions allow producing a variety of nanostructured and amorphous materials, as well as they are advantageous for chemical processes. Ultrasound requires inexpensive equipment and fewer steps than conventional methods. Combining ultrasound and photocatalysis enhances the performance of the processes, reduces reaction time, avoids the use of extreme physical conditions and improves the photocatalytic materials properties increasing their activity. Here, we reported the positive effect of US in synthesizing Me-modified TiO_2 (Me = Ag, Cu, Mn) for pollutants degradation in gas-phase; also, we proved the advantageous application of ultrasound for the photocatalytic removal of organic compounds in water. Ultrasound produced more efficient Me-doped TiO_2, which showed higher activity in visible light. When combined with photocatalytic water treatment, the organic compounds degradation and mineralization increases.

1. Introduction

Established processes often require changes in operation in order to reduce disadvantages and get better results and in this respect, novel methods or equipment could lead to a general process improvement. This work presents some advantages of applying ultrasounds (US) in photocatalysis. US can be used for the synthesis of TiO_2-based catalysts, improving their properties [1]. In addition, US combined with photocatalysis for water treatment speeds up the organic molecules degradation process [2]. Sonochemistry comes from acoustic

cavitation, which concerns formation, growth and collapse of bubbles in a liquid [3]. Collapse generates high-temperature and high-pressure spots, where reactions take place. Extreme conditions underlie the synthesis of nanostructured and amorphous metals, alloys, carbide [4-8], or for example, collapsing bubbles decompose some volatile organometallic compounds, resulting in metal atoms agglomerates [9]. Concerning TiO_2-based catalysts, Pinjari et al. prepared TiO_2 by ultrasound (US) assisted and conventional sol–gel (NUS) synthesis; in this case, the use of ultrasound lowered the temperature required to complete the phase transformation as compared to the conventional approach [10], and also the sonication time affected both crystallinity and crystallite size and of the obtained nanoparticles. Neppolian et al. reported an ultrasound-assisted method for synthesizing nanosized Pt–graphene oxide (GO)–TiO_2 photocatalyst [11], and performed the photocatalytic and sonophotocatalytic degradation of dodecylbenzenesulfonate (DBS) in aqueous solution [12]. Combining photocatalysis with sonochemical oxidation prevented the catalyst aggregation during photocatalysis and the formation of stable H_2O_2 [13], as well as the physical effect of acoustic cavitation kept the catalyst surface constantly clean. Finally, mineralization of DBS was observed to be around 5% higher with sonophotocatalysis than by photocatalytic processes. As far as TiO_2 modification is concerned, in order to enhance its photocatalytic properties, Shirsath et al. doped TiO_2 with Fe and Ce comparing a synthesis by sonochemical approach and conventional doping method [14]; the control over size, morphology and dispersion of the metal components was more difficult in the classical synthesis, and this method often requires longer time and multi-step procedures. On the other hand, acoustic cavitation influenced the properties of doped materials [15], enhancing the surface area, controlling particle size distribution, and finally improving the photocatalytic activity [16, 17].

In the case of the photocatalytic removal of gaseous pollutants, it is well known that it requires visible light active catalysts, and in fact, metal nanoparticles doping TiO_2 extend the absorption wavelengths spectrum.

Among different metals, some of them proved to enhance the properties of TiO_2 in terms of activity under visible light. Plasmonic photocatalysis showed enhanced photocatalytic efficiency in the visible spectrum, increasing the possibility to use sunlight for environmental and energy applications. Plasmonic photocatalysis makes use of noble metal, such as silver. Accordingly, many papers describe the visible light activity of silver doped TiO_2 [18; 19]. On the other hand, less precious and less expensive metals have been investigated, in order to exploit their advantages in terms of cost and availability. Both Cu and Mn show interesting

properties related to light adsorption, photocatalytic activity and interaction with TiO_2-based materials. For example, N. Wu and M. Lee [20] deposited Cu particles on TiO_2, obtaining a significant enhancement in photocatalytic activity for H_2 production from methanol; again, Amoros-Perez et al. [21] reported the photocatalytic decomposition of acetic acid into biogas over different Cu/TiO_2 catalysts, showing higher activity than commercial TiO_2 in all cases. Similarly, Mn as a dopant favors the charge separation [22], and increases the visible light photocatalytic activity of TiO_2 [23]. Hence, we selected Ag, Mn and Cu in order to investigate the effect of US in Me-modified TiO_2 preparation.

On the other hand, water cleaning and purification demand more efficient processes able to degrade cumbersome and persistent molecules. For example, pharmaceuticals are continuously introduced in the aquatic environment [24] and they easily persist because sewage treatments plants are not able to completely remove them. Thus, most urban wastewater contains medicinal compounds [25], representing a real risk for the ecosystem. Advanced oxidation processes (AOPs), such as photocatalysis, are widely applied for water disinfection, and even ultrasound received increasing attention in this sense. Ultrasound requires inexpensive equipment and often fewer steps than conventional methods [26]. Combining ultrasound and photocatalysis is a good opportunity to reduce reaction time without the need for extreme physical conditions [27]. For example, Saien et al. [28] enhanced the photocatalytic degradation rate of styrene-acrilic acid copolymer by ultrasonic irradiation; a degradation of 96 % and mineralization conversion of 91 % were respectively achieved.

Here, we reported the positive effect of US in synthesizing Me-modified TiO_2 (Me = Ag, Cu, Mn) for pollutants degradation in gas-phase, as well as its advantages in treating organic compounds in water.

2. Materials and methods

Commercial TiO_2 (1077, KRONOS Worldwide, Inc.) consists of pure anatase and particles with a diameter ranging between 110 and 130 nm. A thorough characterization is reported elsewhere [29]. Ti(IV)-butoxide (Ti(IV)-BuOX, reagent grade, 97%), nitric acid (HNO_3, ACS reagent, 70%), and ethanol (EtOH, absolute, for HPLC, ≥98%) were purchased from Sigma Aldrich and used without any further treatment. Metal precursors consisted of silver nitrate

($AgNO_3$, ACS Reagent, ≥99%), copper chloride ($CuCl_2*2H_2O$, >99% Sigma Aldrich), and manganese (II) nitrate hydrate ($Mn(NO_3)_2 \cdot xH_2O$, 98%), respectively.

Sonication occurred by a Bandelin SONOPLUS HD 3200 ultrasound generator with a nominal power of 200 W, equipped with a sonication horn (fixed frequency: 20 kHz). The horn tip diameter was 13 mm, thus resulting in a power of 30 W cm^{-2}. A Perkin Elmer Optima 8300 instrument carried out the ICP/OES analysis. The samples were first mineralized by nitric acid followed by microwave treatment.

2.1 Ag-TiO_2 by US

Besides the Ag source, reagents were polyvinylpyrrolidone (PVP40, average mol wt 40,000) and sodium borohydride ($NaBH_4$, ≥99%).

We followed the synthesis reported by Goharshadi et al. as reference [30]. A first solution containing $AgNO_3$, polyvinyl pyrrolidone (PVP40, surfactant) and TiO_2 was mixed by US for 10 min before adding a $NaBH_4$ solution (0.1 M). After the reduction reaction, sonication lasted for 60 min. After the US treatment, the suspension was washed with distilled water and dried at 100 °C.

2.2 Cu-TiO_2 by US

Tao et al. [31] synthesized copper microcrystals by US; this method was selected as reference for Cu NPs deposition on TiO_2. A solution containing L-ascorbic acid as reducing agent, CTAB as surfactant, H_2O and TiO_2 was mixed with a second one composed by $CuCl_2 * 2H_2O$ and NH_3 to adjust the pH. US provided a power of 50 W cm^{-2} for 2.5 h, maintaining the flask at 62 ° C: the sample was then centrifuged and washed, dried and calcined at 400 °C for 2 h.

2.3 Mn-TiO_2 by US

A modified sol-gel US assisted method was employed in the case of Mn promoted materials. $Mn(NO_3)_2$ was first dissolved in water, then HNO_3, EtOH and Ti(IV)-buOX were added. This solution was mixed either by mechanical stirring or submitted to a continuous US irradiation at 40 W cm^{-2}. Temperature was set at 80 °C. Again, drying occurred at 100 °C overnight, and samples were calcined at 400 °C for 2 h.

2.4 Classical Impregnation synthesis

We synthesized other two samples consisting in Ag- and Mn- promoted TiO_2 prepared by classical impregnation, without ultrasound. The classical TiO_2 impregnation occurred in a Rotavapor apparatus. TiO_2 was added firstly followed by the aqueous solution of the metals precursor. Suspension blending lasted 24 h at 40 °C, then other 2 h at 80 °C. Samples were dried overnight at 100 °C and then calcined at 400 °C for 2 h.

2.5 Amount of Metals

The relative amounts of TiO_2 and metal precursor of each sample is reported in table 1.

Sample	Method	Support	Me precursor	TiO_2/Me
Ag-TiO_2_US	Impregnation + US	TiO_2 (1077)	$AgNO_3$	2/0.2 w/w
Cu-TiO_2_US	Impregnation + US	TiO_2 (1077)	$CuCl_2$*$2H_2O$	2/0.2 w/w
Mn-TiO_2_US	US-assisted sol gel synthesis	Ti(IV)-buOX	$Mn(NO_3)_2$	5/1 mol/mol
Ag-TiO_2 (NO US)	Classical impregnation	TiO_2 (1077)	$AgNO_3$	1/0.1 w/w
Mn-TiO_2 (NO US)	Classical impregnation	TiO_2 (1077)	$Mn(NO_3)_2$	1/0.2 w/w

Table 1. Sample list with relative amounts of TiO_2 and Me.

The specific metal amount has been chosen based on previous researches, which provided an optimization of the catalyst according with the Me loading.

2.6 Characterization analyses

XRD spectra were collected using a PW 3830/3020 X' Pert Diffractometer from PANalytical working Bragg-Brentano, using the Cu Kα1 radiation (k = 1.5406 Å). High-resolution transmission electron microscopy (HR-TEM) images were collected using a JEOL 3010-UHR Instrument (acceleration potential 300 kV; LaB_6 filament), equipped with an Oxford INCA X-ray energy dispersive spectrometer (EDS) with a Pentafet Si(Li) detector. Samples were ''dry'' dispersed onto lacey carbon Cu grids.

2.7 Photocatalytic tests in gas phase

The photodegradation of model molecules (Acetone, HPLC Plus ≥99.9% Sigma-Aldrich; Ethanol, absolute, for HPLC, ≥99.8%, Sigma-Aldrich) occurred in a Pirex glass reactor (5 L). The catalyst was deposited as a thin film on a glass support. We suspended the powder in isopropanol and then we spread three layers of it on the glass surface. A micro-GC (Agilent 3000 A micro-GC) was directly connected to the reactor and automatically analyzed the organics concentration. This setup is also described elsewhere [32].

The source of irradiation was visible light (LED, MW mean well, 350mA rated current, 9–48V DC voltage range, 16.8 W rated power). Lamps distance resulted in intensity equal to 15,000 lux.

2.8 Sono-Photocatalysis in liquid phase

We studied the degradation of two reference drugs, i.e Ibuprofen (≥98% (GC), Sigma-Aldrich) and Acetaminophen (BioXtra, ≥99.0%, Sigma-Aldrich).

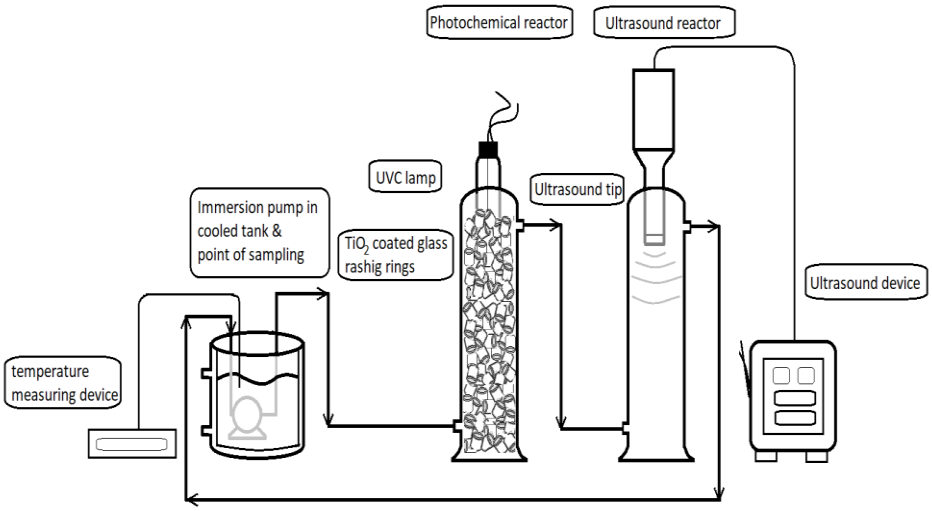

Figure 1. Setup for liquid-phase sono-photodegradation of drugs.

Reactions occurred in a continuous system provided with two glass cylindrical reactors (500 ml), one for the TiO_2 photocatalytic treatment and the other for drugs ultrasonic degradation (Fig. 1). The photocatalytic reactor contained a UV-C immersion lamp (germicidal 9 W UV-C lamp purchased from Jelosil) providing an irradiation of 55 W m^{-2}, and was filled with TiO_2-coated glass Raschig rings (Ø = 8 mm; total geometrical area = 0.23 m^2). The ultrasonic horn was immersed in the second cylindrical reactor (Sonix GEX500, 20 kHz). Starting concentration of organics was 20 ppm. The total volume was 2 L, recirculating in the system with a controlled flow rate of 90 L h^{-1}. We followed the reaction kinetic by sampling every hour for 6 hours. HPLC (High Performance Liquid Chromatography) analyses were performed using Agilent 1100 Series Instrument, a diode array detector and with a 125 mm × 4 mm C18 reverse-phase column, following the pharmaceutical compounds degradation and providing their concentration profiles over time. The mineralization percentage was determined through the Total Organic Carbon (TOC) content. TOC was measured with a 5000 A Shimadzu instrument.

3. Results and discussion

Ultrasound acts on the NPs formation, and at the same time, it enhances their distribution on TiO_2 surface. In fact, US induce a faster solute diffusion, and can affect the interaction between metal NPs and the surfactant during the particles' growth, thus influencing the morphology.

3.1 Photocatalytic activity of Me-modified TiO_2 by US

Visible light wavelengths (400 – 700 nm) are not able to excite TiO_2 electrons from the valence band to the conduction band. Thus, TiO_2 photocatalytic degradation of VOC in gas-phase under visible light is completely ineffective, as already reported [33].

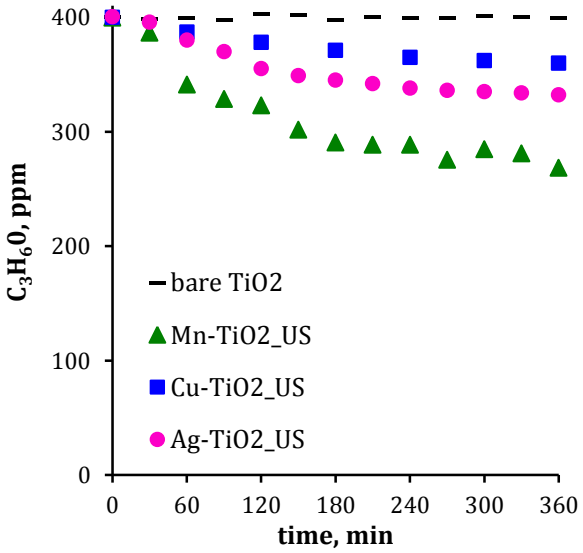

Figure 2. Acetone (C° = 400 ppm) degradation over time. Comparison between bare-TiO_2 and Me-doped TiO_2 by US assisted syntheses. Visible light irradiation (LED). Temperature constant at 25 °C. 40 % RH.

The increase in visible-light absorption due to the presence of metal species resulted in enhanced photocatalytic activity for all the metals (Fig. 2). Activity under visible light was ascribable to Ag NPs capability of absorb light with wavelengths above 400 nm, because of the plasmonic resonance. Electron transfer may occur from Ag to TiO_2, increasing the number of electron that can react. Subsequently, the concentration of photo-generated species is higher at the TiO_2 surfaces increasing the possibility of having oxidation or reduction reactions. A previous work already reported the correlation between the presence of Cu and the absorption of visible wavelengths by copper-modified TiO_2 samples [32]; the presence of copper also affected the band gap. In this case, the photocatalytic behavior can be related both to the presence of Cu metal NPs and to some cupric oxide species. Again, metal NPs take

visible light electrons acting as electron traps and reducing electrons-hole recombination rate [34]. On the other hand, even the presence of CuO and Cu_2O is important, due to the formation of an heterojunction between TiO_2 and CuO first, and the formation of the system Cu_2O–CuO, where it is possible to have an electron transfer from Cu_2O to CuO [35]. In a similar way, Mn and MnO_2 species doping TiO_2 may act as electrons traps [36], improve the e^-/h^+ separation and decrease the band gap [37]. The higher degradation obtained by Mn-TiO_2 was due to the higher surface area, being Mn-TiO_2 nanometric (see also TEM images, Fig. 7).

3.1.1 Mn-TiO_2 prepared with and without US

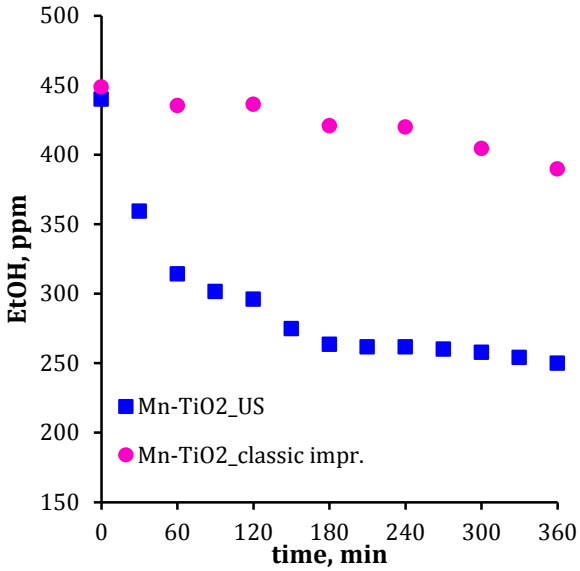

Figure 3. EtOH (C° = 450 ppm) degradation over time by M-TiO_2 synthesized by classic impregnation (•) and US-assisted method (■). Visible light irradiation (LED). Temperature constant at 25 °C. 40% RH.

We firstly tried to support Mn on commercial TiO_2 by classical impregnation. In this case, we have a negligible interaction between the metal and the support due to the simple decoration of the Mn at the TiO2 surface. Considering the TiO_2 alone is not active under pure LED light (Fig.2), the presence of the Mn does not improve the photocatalyst efficiency in a satisfactory way (Fig. 3). The addition of manganese was advantageous only when it was added during the TiO_2 synthesis giving an *in-situ* doping. For the reason we decided to investigate the potential of US, applying it directly on the classical sol-gel synthesis, as described in the experimental part (see par. 2.3). Here, US efficiently improved the sample properties resulting in enhanced photocatalytic activity under visible light (Fig. 3).

3.1.2 Ag-TiO_2 prepared with and without US

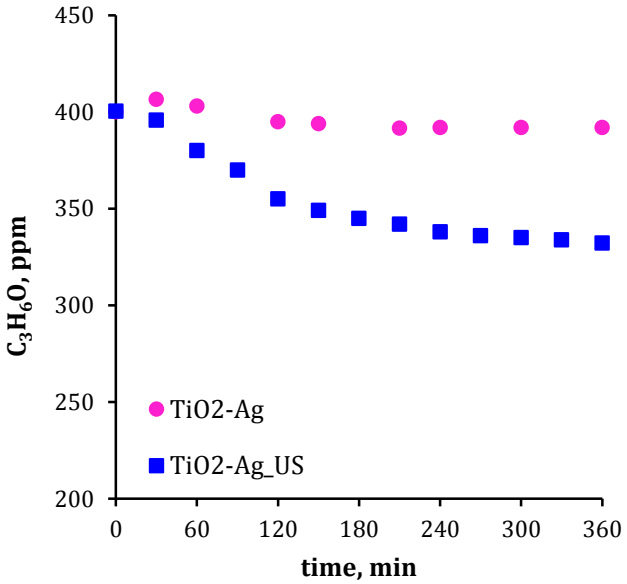

Figure 4. Acetone (C° = 400 ppm) degradation over time by Ag-TiO_2 synthesized by classic impregnation (•) and US-assisted method (■). Visible light irradiation. Temperature constant at 25 °C. 40 % RH.

Ag was deposited on commercial TiO_2 by classical impregnation and by US-assisted impregnation. In this case US were advantageous to deposit Ag NPs on the surface of the commercial TiO_2. Ag-TiO_2 by US degraded acetone under visible light accordingly with the particular morphology of silver NPs due to sonication (see the characterization part). Concerning this, we already described the specific effect of US for TiO_2 impregnation [38].

3.3 Morphological characterization

As far as the morphological features of the TiO_2 support (1077 by Kronos) is concerned, its particles result in no difference whether they were plain or US-treated for impregnation: in fact, the particles maintain both their shape and size typical of a micrometric titania material [39].

When Ag is supported by classical impregnation onto TiO_2 (see figure 5, left-hand section), it is evident that besides the main features, typical of micrometric titania, which is made up of large and ordered anatase microcrystals (both the fringes inspection and the diffraction pattern indicate the usual d_{hkl} belonging to the (101) distance - 0.352 nm (ICDD n. 21-1272), see the smaller inset in the figure), there is a very faint distribution of nano-disperse Ag particles, ranging from 0.5 to 2 nm (see the larger inset in the left-hand section).

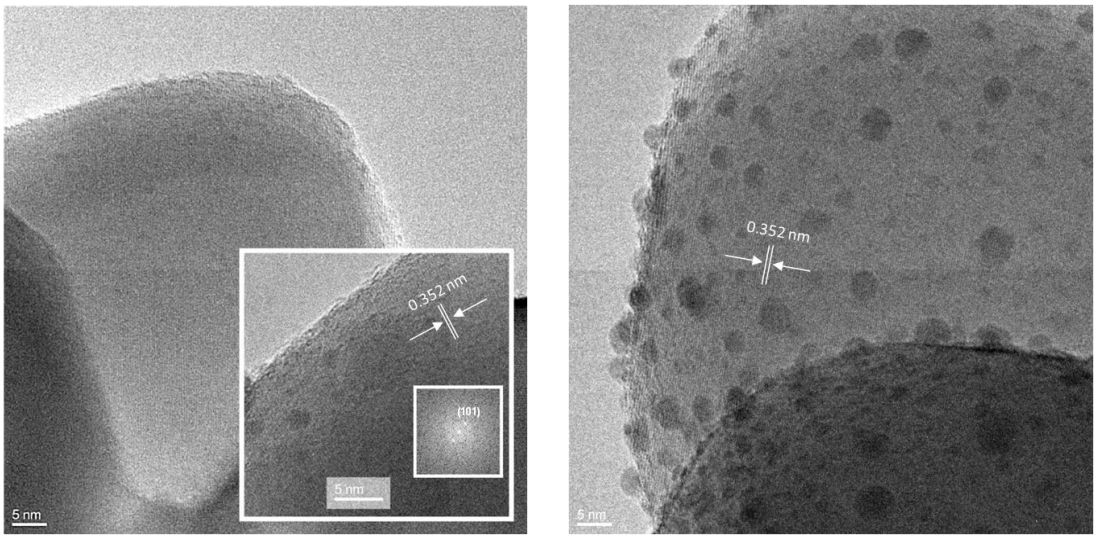

Figure 5. Ag-TiO_2 synthesised by classical impregnation withous (left) or with (right) ultrasound during impregnation

On the contrary, in the case of US-assisted synthesis of Ag-TiO_2 a huge amount of homogeneously distributed Ag nano-particles (NPs) on TiO_2 surface are present (see Figure 5, right-hand section) and their dimension span in a 2-5 nm range. TEM images thus confirm the positive effect of applying US during the impregnation in order to obtain a large amount of Ag NPs in a definite dimension range, also confirming that the micrometric support totally retains its morphological features.

In order to confirm the positive effect of US in the realisation of a real surface decoration of TiO_2 by means also of other metal NPs, we decided to employ Cu species, as already proposed in the literature and in a previous paper by our same research group [32, 40].
HR-TEM characterization of the Cu-promoted micrometric titania are reported in Figure 6: it is again well evident that the TiO_2 support has undergone no morphological change upon US treatment, whilst the presence of Cu species is clearly documented by the presence of both single (nano)particles, exhibiting average dimensions in the 2.5 nm range, and aggregates of much larger sizes (see the inset to Figure 6).

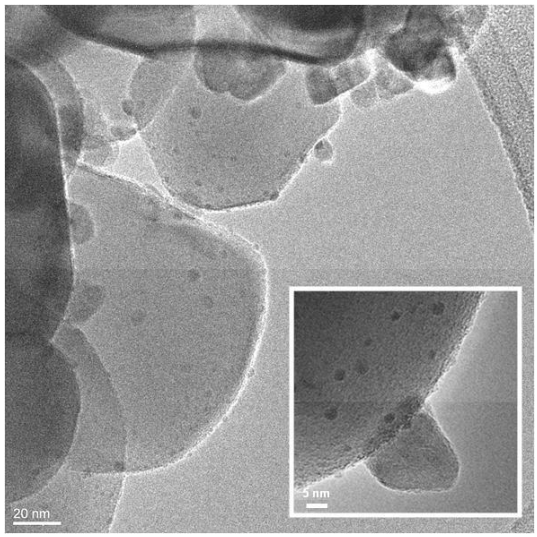

Figure 6. HR-TEM images of Cu-TiO_2 synthetized by US assisted impregnation method.

In order to investigate the role played by US in the general approach to obtain a promotion on the photocatalytic properties of TiO_2, we set aside the employ of the micrometric system by Kronos, deciding to proceed with a classical one-step sol-gel preparation of titania with Mn species as promoters and enhanced by the use of US.

Mn-TiO_2 prepared by this procedure resulted in a nanometric TiO_2 presenting roundish particles with average size dimensions in the 5-7 nm range: see the left-hand side of Figure 7. Both anatase and rutile (even to a minor extent) polymorphs of TiO_2 have been identified based on the fringe patterns and electronic diffraction: this evidence well agrees with literature data as well [41].

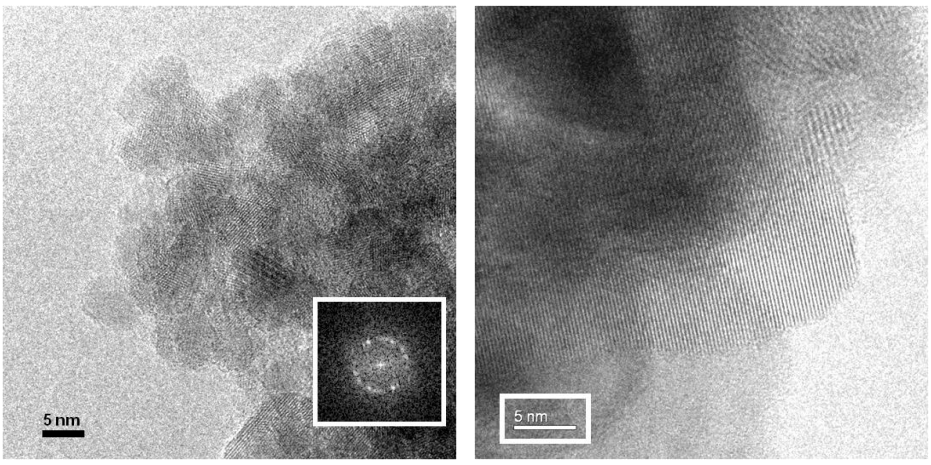

Figure 7. HR TEM of Mn-TiO_2 prepared by US-modified sol-gel method.

Moreover, the presence of Mn species is assessed by the EDS analysis (not reported for the sake of brevity): in fact, randomly ordered oxidic nanoparticles (average size dimensions in the 10-20 nm range) made up of either Mn_2O_3 or Mn_3O_4, as witnessed by the analyses of the fringe patterns, are well observable in the right-hand section of Figure 7. Once more, the inspection of both fringe patterns and electronic diffraction confirms the qualitative information coming from EDS results, indicating that it is possible to identify here and there (i) the (222) family planes belonging to Mn_2O_3 in the bixbyite form (ICDD n. 41-1442) or (ii) the (112) family planes belonging to Mn_3O_4 in the hausmannite form (ICDD n. 2-1062). These features are again in good agreement with what reported in [42].

3.4 Sono-photocatalytic degradation in liquid phase

Sonolysis resulted in ibuprofen degradation lower than 8 %, without mineralization (Fig. 8). On the contrary, UV-C photolysis partially converted the substrate and mineralized it up to 25 %. However, the contribution of TiO_2 was clearly proved considering that ibuprofen degradation increased from 71 % to 92 %, together with the mineralization that reached 28 %.

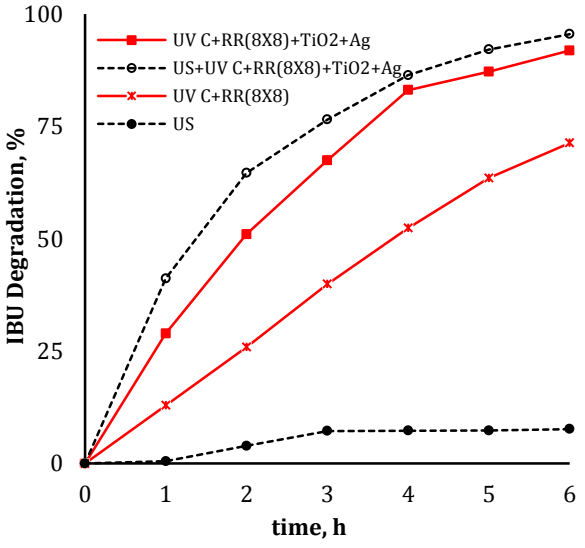

Figure 8. Ibuprofen (IBU) degradation over time. Comparison between sonolysis (US), photolysis (UV-C), photocatalysis (UV-C+TiO_2-Ag) and sono-photocatalysis (US+UV-C+TiO_2-Ag).

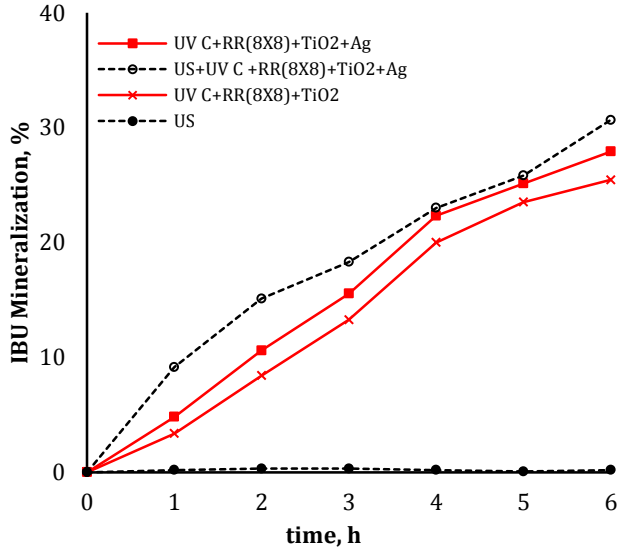

Figure 9. Ibuprofen (IBU) mineralization.

The catalyst was TiO_2-Ag considering its higher performance in liquid phase if compared with naked TiO_2 or TiO_2 modified with other metals. The application of US definitely improved the

reaction kinetics, converting more than 95 % of ibuprofen and mineralizing more than 30 % in 6 h (Fig. 9). Considering the mineralization-increasing trend, in case of sono-photocatalytic treatment, it showed that mineralization might continue proceeding with the reaction, since the curve did not reach a plateau.

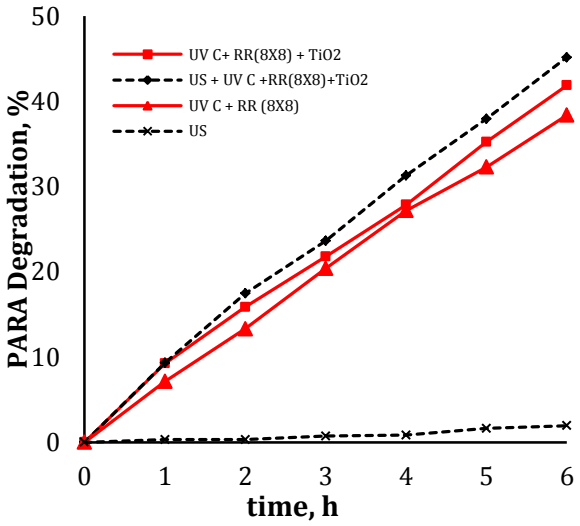

Figure 10. Paracetamol (PARA) degradation over time. Comparison between sonolysis (US), photolysis (UV-C), photocatalysis (UV-C+TiO_2-Ag) and sono-photocatalysis (US+UV-C+TiO_2-Ag).

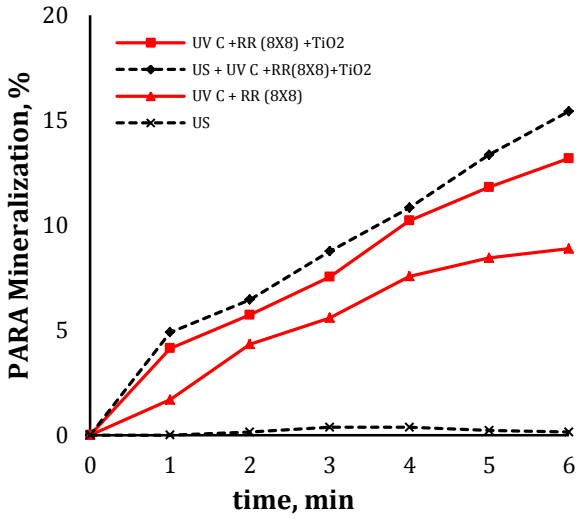

Figure 11. Paracetamol (PARA) mineralization.

Changing the substrate, the trend was similar (Fig. 10 and Fig. 11). Again, sonolysis did not convert paracetamol; however, the contribution of photolysis was rather high, reaching only by UV-C irradiation a paracetamol conversion of 38 %, with 9 % of mineralization. If the further contribution of TiO_2 and US did not drastically improve the total substrate conversion, their effect was more evident considering the final mineralization. Indeed, it increased from 8 % to 16 % applying US and TiO_2 as photocatalyst. In this case, the mineralization trend assumes that it constantly increases as the reaction continues.

Conclusion

US can be applied in photocatalysis both for improving the TiO_2-based materials synthesis and reaction kinetics. Doping TiO_2 with Cu, Mn or Ag resulted in higher visible-light activity when syntheses occurred under sonication. Cu-TiO_2, Mn-TiO_2 and Ag-TiO_2 by US efficiently converted acetone to CO_2 under visible light. In particular, US allowed depositing either Cu or Ag on the surface of a commercial and pigmentary TiO_2. This latter may easily be used for

photocatalytic building materials, being safe (metal nanoparticles are supported and immobilized, while the support in micrometric), cheap and working under solar or visible-light. On the other hand, US clearly enhanced the photocatalytic abatement of organic contaminants in water. Combining UV light, Ag-TiO_2 and US completely degraded ibuprofen or paracetamol in water, showing rather good level of mineralization. Further toxicological test can demonstrate that the treatment reduces the final toxicity improving the quality of water.

Acknowledgements

This work is dedicated to the memory of Mrs. Benedetta Sacchi.

References

[1] K. S. Suslick, T. Hyeon, M. Fang, Nanostructured Materials Generated by High-Intensity Ultrasound: Sonochemical Synthesis and Catalytic Studies, Chem. Mater. 8(8) (1996) 2172–2179.

[2] Y. G. Adewuyi, Sonochemistry in Environmental Remediation. 2. Heterogeneous Sonophotocatalytic Oxidation Processes for the Treatment of Pollutants in Water, Environ. Sci. Technol. 39(22) (2005) 8557–8570.

[3] K. S. Suslick, In: K. S. Suslick (Ed.), Ultrasound: Its Chemical, Physical, and Biological Effects, VCH Press: New York, 1988, p. 123.

[4] K. S. Suslick, Applications of Ultrasound to Materials Chemistry, MRS Bull. 20 (1995), 29-34.

[5] K. S. Suslick, Ultrasound: Applications to Materials Chemistry, In: R. W. Cahn (Ed.), Encyclopedia of Materials Science and Engineering, Pergamon Press: Oxford, 1993, pp. 2093-2098.

[6] K. S. Suslick, T. Hyeon, M. Fang, A. A. Cichowlas, Sonochemical synthesis of nanostructured catalysts, Mater. Sci. Eng. A 204 (1995) 186-192.

[7] K. S. Suslick, S. B. Choe, A. A. Cichowlas, M. W. Grinstaff, Sonochemical Synthesis of Amorphous Iron, Nature 353 (1991) 414-416.

[8] T. Hyeon, M. Fang, K. S. Suslick, Nanostructured Molybdenum Carbide: Sonochemical Synthesis and Catalytic Properties, J. Am. Chem. Soc. 118 (1996), 5492-5493.

[9] K. S. Suslick, M. Fang, T. Hyeon, Sonochemical Synthesis of Iron Colloids,J. Am. Chem. Soc. 118 (1996) 11960-11961.

[10] D.V. Pinjari, K. Prasad, P.R. Gogate, S.T. Mhaske, A.B Pandit, Synthesis of titanium dioxide by ultrasound assisted sol–gel technique: Effect of calcination and sonication time, Ultrason. Sonochem. 23 (2015) 185-191.

[11] H. Zhang, X. Lv, Y. Li, Y. Wang, J. Li, P-25 Graphene composite as a high performance photocatalyst, ACS Nano 4 (2010) 380-386.

[12] B. Neppolian, A. Bruno, C. L. Bianchi, M. Ashokkumar, Graphene oxide based Pt–TiO2 photocatalyst: Ultrasound assisted synthesis, characterization and catalytic efficiency, Ultrason. Sonochem. 19(1) (2012), Pages 9-15.

[13] E. Selli, C.L. Bianchi, C. Pirola, G. Cappelletti, Efficiency of 1,4-dichlorobenzene degradation in water under photolysis photocatalysis on TiO2 and sonolysis, J. Hazard. Mater. 153 (2008) 1136-1141.

[14] S.R. Shirsath, D.V. Pinjari, P.R. Gogate, S.H. Sonawane, A.B. Pandit, Ultrasound assisted synthesis of doped TiO2 nano-particles: Characterization and comparison of effectiveness for photocatalytic oxidation of dyestuff effluent, Ultrason. Sonochem. 20(1) (2013) 277-286.

[15] M. Zhou, J. Yu, B. Cheng, Effects of Fe-doping on the photocatalytic activity of mesoporous TiO2 powders prepared by an ultrasonic method, J. Hazard. Mater. B137 (2006) 1838-1847.

[16] X.K. Wang, C. Wang, W.L. Guo, Sonochemical synthesis of nitrogen doped TiO2 at a low temperature, Adv. Mater. Res. 356 (2012) 403-406;

[17] J. Yu, M. Zhou, B. Cheng, H. Yu, X. Zhao, Ultrasonic preparation of mesoporous titanium dioxide nanocrystalline photocatalysts and evaluation of photocatalytic activity, J. Mol. Catal. A: Chem. 227 (2005) 75-80.

[18] M. K. Seery, R. George, P. Floris, S. C. Pillai, Silver doped titanium dioxide nanomaterials for enhanced visible light photocatalysis, J. Photochem. Photobiol. A: Chem. 189 (2007) 285-263.

[19] Q. Xiang, J. Yu, B. Cheng, H. C. Ong, Microwave-Hydrothermal Preparation and Visible-Light Photoactivity of Plasmonic Photocatalyst Ag-TiO_2 Nanocomposite Hollow Spheres, Chem. Asian J. 5 (2010) 1466 – 1474.

[20] N.Wu, M. Lee, Enhanced TiO2 photocatalysis by Cu in hydrogen production from aqueous methanol solution, Int. J. Hydrogen En. 29 (2004) 1601-1605.

[21] A. Amorós-Pérez, L. Cano-Casanova, M. Lillo-Ródenas, M. Carmen Román-Martínez, Cu/TiO_2 photocatalysts for the conversion of acetic acid into biogas and hydrogen, Catal. Today 287 (2017) 78-84.

[22] L.G. Devi, N. Kottam, S.G. Kumar, Preparation and characterization of Mn-doped titanates with a bicrystalline framework: correlation of the crystallite size with the synergistic effect on the photocatalytic activity, J. Phys. Chem. C, 113 (2009), 15593-15601.

[23] Q.R. Deng, X.H. Xia, M.L. Guo, Y. Gao, G. Shao Mn-doped TiO_2 nanopowders with remarkable visible light photocatalytic activity Mater. Lett., 65 (13) (2011) 2051-2054.

[24] K. Kümmerer, The presence of pharmaceuticals in the environment due to human use - present knowledge and future challenges, J. Environ. Manage 90 (2009) 2354-2366.

[25] O.A.H. Jones, N. Voulvoulis, J.N. Lester, Human pharmaceuticals in wastewater treatment processes, Crit. Rev. Environ. Sci. Technol. 35 (2005) 401-427.

[26] C. Sullivan, Sonochemistry—a sound investment, Chem. Ind. 18 (1992) 365-367.

[27] C.G. Joseph, L.P. Gianluca, B. Awang, D. Krishnaiah, Sonophotocatalysis in advanced oxidation process: a short review, Ultrason. Sonochem. 16 (2009) 583-589.

[28] J. Saien, H. Delavari, A.R. Solymani, Sono-assisted photocatalytic degradation of styrene-acrylic acid copolymer in aqueous media with nano titania particles and kinetic studies, J. Hazard. Mater. 177(1–3) (2010) 1031-1038.

[29] C.L. Bianchi, S. Gatto, C. Pirola, A. Naldoni, A. Di Michele, G. Cerrato, V. Crocellà, V. Capucci, Photocatalytic degradation of acetone, acetaldehyde and toluene in gas- phase: comparison between nano and micro-sized TiO2, Appl. Catal. B: Environ. 146 (2014) 123–130.

[30] E.K. Goharshadi, H. Azizi-Toupkanloo, Silver colloid nanoparticles: ultrasound-assisted synthesis, electrical and rheological properties, Powder Technol. 237 (2013) 97–101.

[31] X. Tao, Y. Zhao, Sonochemical synthesis and characterization of disk-like copper microcrystals, Mater. Chem. Phys. 125 (2011) 219–223.

[32] M. Stucchi, C. L. Bianchi, C. Pirola, G. Cerrato, S. Morandi, C. Argirusis, G. Sourkouni, A. Naldoni, V. Capucci, Copper NPs decorated titania: A novel synthesis by high energy US with a study of the photocatalytic activity under visible light, Ultrason Sonochem. 31 (2016) 295-301.

[33] M. Stucchi, C.L .Bianchi, C.Pirola, S. Vitali, G. Cerrato, S. Morandi, C. Argirusis, G. Sourkouni, P.M. Sakkas, V.Capucci, Surface decoration of commercial micro-sized TiO_2 by means of high energy ultrasound: A way to enhance its photocatalytic activity under visible light, Appl. Catal. B Env. 178 (2015) 124–132.

[34] A. Kubacka, M.J. Munoz-Batista, M. Ferrer, M. Fernandez-Garcia, UV and visible light optimization of anatase TiO_2 antimicrobial properties: surface deposition of metal and oxide (Cu, Zn, Ag) species, Appl. Catal. B 140–141 (2013) 680– 690.

[35] P. Wang, X. Wen, R. Amal, Y. Hau, Introducing a protective interlayer of TiO2 in Cu2O–CuO heterojuction thin film as a highly stable visible light photocathode, RCS Adv. 5 (2015) 5231–5236.
[36] W. Zhang, Y. Liu, B. Yu, J. Zhang, W. Lian, Effects of silver substrates on the visible light photocatalytic activities of copper-doped titanium dioxide thin films, Mater. Sci. Semicond. Process. 30 (2015) 527–534.
[37] M. C. Nevárez-Martínez, M. P. Kobylański, P. Mazierski, J. Wółkiewicz, G. Trykowski, A. Malankowska, M. Kozak, P. J. Espinoza-Montero, A. Zaleska-Medynska, Self-Organized TiO_2–MnO_2 Nanotube Arrays for Efficient Photocatalytic Degradation of Toluene, Molecules 22 (2017) 564-578.
[38] M. Stucchi, C.L. Bianchi, C. Argirusis, V. Pifferi, B. Neppolian, G. Cerrato, D.C. Boffito, Ultrasound assisted synthesis of Ag-decorated TiO2 active in visible light, Ultrason. Sonochem. 40 (2018) 282–288.
[39] C.L. Bianchi, S. Gatto, C. Pirola, A. Naldoni, A. Di Michele, G. Cerrato, V. Crocellà, V. Capucci, Photocatalytic degradation of acetone, acetaldehyde and toluene in gas- phase: comparison between nano and micro-sized TiO_2, Appl. Catal. B: Environ. 146 (2014) 123–130.
[40] G. Colón, M. Maicu, M.C. Hidalgo, J.A. Navío, Cu-doped TiO2 systems with improved photocatalytic activity, Appl. Catal. B Env. 67(1–2) (2006) 41-51.
[41] M. Stucchi, A. Elfiad, M. Rigamonti, H. Khan, D.C. Boffito, Water treatment: Mn-TiO_2 synthesized by ultrasound with increased aromatics adsorption, Ultrason. Sonochem. 44 (2018) 272-279.